



Since January 2020 Elsevier has created a COVID-19 resource centre with free information in English and Mandarin on the novel coronavirus COVID-19. The COVID-19 resource centre is hosted on Elsevier Connect, the company's public news and information website.

Elsevier hereby grants permission to make all its COVID-19-related research that is available on the COVID-19 resource centre - including this research content - immediately available in PubMed Central and other publicly funded repositories, such as the WHO COVID database with rights for unrestricted research re-use and analyses in any form or by any means with acknowledgement of the original source. These permissions are granted for free by Elsevier for as long as the COVID-19 resource centre remains active.



## Impact of quarantine on fractional order dynamical model of Covid-19

Ram Singh<sup>a,\*</sup>, Prayag Tiwari<sup>b,\*</sup>, Shahab S. Band<sup>c,\*</sup>, Attiq U. Rehman<sup>a</sup>, Shubham Mahajan<sup>e,f,d</sup>,  
Yijie Ding<sup>g</sup>, Xiaobin Liu<sup>h,\*</sup>, Amit Kant Pandit<sup>d</sup>

<sup>a</sup> Baba Ghulam Shah Badshah University Rajouri, 185234, India

<sup>b</sup> School of Information Technology, Halmstad University, Sweden

<sup>c</sup> Future Technology Research Center, College of Future, National Yunlin University of Science and Technology, Douliou, Taiwan, ROC

<sup>d</sup> School of Electronic and Communication, Shri Mata Vaishno Devi University, Katra, 182320, India

<sup>e</sup> Ajeenkya D Y University, Pune, Maharashtra, India

<sup>f</sup> iNurture Education Solutions Pvt. Ltd., Bangalore, India

<sup>g</sup> Yangtze Delta Region Institute (Quzhou), University of Electronic Science and Technology of China, Quzhou, 324000, China

<sup>h</sup> Department of Nephrology, The Affiliated Wuxi People's Hospital of Nanjing Medical University, 214023, Wuxi, China

### ARTICLE INFO

#### Keywords:

Equilibria points  
Existence and uniqueness  
Ulam–Hyers stability  
Numerical simulations

### ABSTRACT

In this paper, a Covid-19 dynamical transmission model of a coupled non-linear fractional differential equation in the Atangana-Baleanu Caputo sense is proposed. The basic dynamical transmission features of the proposed system are briefly discussed. The qualitative as well as quantitative results on the existence and uniqueness of the solutions are evaluated through the fixed point theorem. The Ulam-Hyers stability analysis of the suggested system is established. The two-step Adams-Bashforth-Moulton (ABM) numerical method is employed to find its numerical solution. The numerical simulation is performed to access the impact of various biological parameters on the dynamics of Covid-19 disease.

### 1. Introduction

As per the report of International Committee on Taxonomy of Viruses, the Coronavirus disease 2019 (Covid-19) are single standard, enveloped and non-segmented Ribonucleic acid virus which belongs to the family of Nidovirales and Coronaviridae [1]. Coronavirus disease 2019 formerly known as Severe Acute Respiratory Syndrome Coronavirus 2 (SARS-CoV-2) or 2019-nCoV caused an outbreak of unusual pneumonia, which is now officially identified as Covid-19 by the World Health Organization (WHO). The Covid-19 virus was first observed in Wuhan, Hubei province of China in December 2019 and after quickly spreading throughout the world [2]. On the 30th of January 2020, the WHO declared it an outbreak and after that on the 11th of March 2020, they said it was a pandemic due to its high rate of infection [3]. Further, this outbreak is resulting in an epidemic throughout the world [4–6]. Globally, as of 22nd February 2022, there has been approximately forty-two crore confirmed number of Covid-19 virus cases including 58,90,312 fatalities, recorded by WHO [3].

#### 1.1. Covid-19 associated symptoms and effects

The coronavirus disease shows effects on human populations in different methods. The most infected population will develop mild to intermediate diseases. Covid-19 has the most common symptoms like cough, tiredness, fever and loss of smell or taste. Its less common symptoms are headache, diarrhea, sore throat, pains, aches, irritated or red eyes, discoloration of toes or fingers and rashes on the skin. Also, its serious signs include loss of speech, loss of mobility, loss of confusion, shortness or trouble breathing and chest pain. These symptoms normally arise over the human population from time to time for weather movement. The high rate of infected population recovering from the ailment without any kind of medical equipment [7,8]. The human population's physiological aging medical problems are high blood pressure, respiratory, heart difficulties, diabetes, sugar patient, infected mosquitoes affected people and weakened body systems should be given more attention. This population is at a higher risk of developing a serious kind of disease.

\* Corresponding authors.

E-mail addresses: [drramsinghmaths@gmail.com](mailto:drramsinghmaths@gmail.com) (R. Singh), [prayag.tiwari@ieee.org](mailto:prayag.tiwari@ieee.org) (P. Tiwari), [shamshirbands@yuntech.edu.tw](mailto:shamshirbands@yuntech.edu.tw) (S.S. Band), [attiqrehman24@gmail.com](mailto:attiqrehman24@gmail.com) (A.U. Rehman), [mahajanshubham2232579@gmail.com](mailto:mahajanshubham2232579@gmail.com) (S. Mahajan), [wuxi\\_dyj@163.com](mailto:wuxi_dyj@163.com) (Y. Ding), [viplxb163@163.com](mailto:viplxb163@163.com) (X. Liu), [amitkantpandit@gmail.com](mailto:amitkantpandit@gmail.com) (A.K. Pandit).

<https://doi.org/10.1016/j.complbiomed.2022.106266>

Received 29 August 2022; Received in revised form 12 October 2022; Accepted 30 October 2022

Available online 9 November 2022

0010-4825/© 2022 The Author(s). Published by Elsevier Ltd. This is an open access article under the CC BY license (<http://creativecommons.org/licenses/by/4.0/>).

When a susceptible person speaks, sneezes, sings, coughs, or breathes noisily, tiny droplets issuing from nose or mouth are exchanged from one person to another, especially in poorly congested and ventilated interior locations when it is impossible to rule out the possibility of small distance mist. Coronavirus disease can also be brought on by coming into contact with infected surfaces or objects and then touching your mouth, nose, eyes, or lips. By some reports, even those who have no signs and symptoms can spread the Covid-19 infection [9]. But, the intensity of spreading such dynamical transmissions of coronavirus are unknown. The maximum index of suspicion is currently being displayed in terms of attentiveness regionally, locally and worldwide. Human population with high fever are currently being tested for coronavirus disease and sent home if the result is negative, indicating that the possibility has been ruled out. If a case is neglected, the ramifications of coronavirus disease might be fatal. Infected populations with a high fever and a Covid-19 infection may be screened [10]. Up to 3.58 people could be affected by a single case of the disease when a patient has a sickness. The frequent use of chloroquine, hydroxychloroquine and other treatments in these areas explains the adverse relationship between coronavirus disease. The effectiveness of chloroquine and hydroxychloroquine in the treatment of infections was examined during the initial SARS outbreak. Some previous research expanded that the utility of hydroxychloroquine in the treatment of SARS-CoV-2, claiming per/day need of 400 mg of hydroxychloroquine for 10 days was the most effective treatment option.

## 1.2. Principles of fractional operators

Since ordinary calculus is extended into fractional calculus. It allows them to the system be better than ordinary calculus. Due to two important reasons that are (i) We can choose any order for the fractional operators, rather than being limited to integer order. (ii) Fractional operators are beneficial when the system has long-term memory since they are dependent not just on local conditions but also on the past. Different types of fractional operators have been proposed in recent research. However, many scholars have employed fractional operators like as Riemann-Liouville, Caputo, Caputo-Fabrizio and Atangana-Baleanu, which have some important and useful operators in both differentiation and integration. Each fractional operator has its own set of benefits and disadvantages. There are numerous benefits and drawbacks to using the Riemann-Liouville fractional operator. From a historical standpoint, the Riemann-Liouville fractional operator is extremely important. The power law is used to calculate the RL fractional derivative. Because of the memory property, it explains real-world situations with a lot of additional information [11]. However, its drawbacks are (i) Fractional operator of the constant function is non-zero in Riemann-Liouville. (ii) The initial condition does not depend on non-fractional order derivatives only. These two shortcomings are overcome by Caputo that is (i) The fractional derivative of constant function is zero. (ii) The initial condition depends on the non-fractional order derivative only. The Caputo fractional derivative has a singular non-local kernel. Before the year 2015, all of the earlier utilized fractional derivatives demonstrate the singular type kernels.

Many scholars have recently become interested in some novel sorts of fractional differentiate operators involve non-singular kernels. To address some of the shortcomings of kernel singularity, Caputo and Fabrizio introduced the fractional operator, which are extension of famous Caputo fractional-order operator to a high abstract associating a non-singular type kernel [12]. However, because of the localized nature of its kernel, the Caputo-Fabrizio derivative has several issues. Atangana and Baleanu presented a fractional operator that associates the Mittag-Leffler function as a non-singular as well as a non-local kernel to solve the problems of locality and singularity of kernels [13]. The fractional operator gives an effective formulation for heredity and memory effects shown in a big area of physical issues when using Mittag-Leffler function as the kernel. The use of fractional operators in the computational

modeling of communicable illnesses isn't a novel concept [14–16]. Several computational models have been developed to better comprehend the disease's dynamic transmission and optimal control [17]. The formulated models in a large number of these studies include non-fractional order derivatives [18–21]. However, in most real-world issues, non-fractional order operators fail to appropriately represent memory and heredity effects. Other academics have extended some of these mathematical models to include non-integer order derivatives. There are several mathematical research on fractional-order Covid-19 models dynamical transmission in there [22]. Many scholars have been interested in the outcomes of investigations on non-integer Covid-19 models [23]. The susceptible, exposed, asymptomatic, symptomatic as well as removed compartments are all included in the fractional-order Covid-19 mathematical model [24]. Additionally, they contend that the behaviour of the system as determined by the stability study is not significantly affected by the memory effects seen in non-integer operators. In the Caputo-Fabrizio in Caputo sense, the Covid-19 system with state variable non-integer order derivative has been investigated [25]. To produce novel existence as well as unique conclusions, the fixed point theory was used. Furthermore, significant results relating to the system's further extended Ulam-Hyers stability have been obtained. Other recent research on non-integer dynamical transmission Models of Covid-19 [26–29]. The effect of differentiation on the dynamical transmission of the illness has been investigated using a numerical scheme therein [30].

In this paper, we have generalized the traditional SEIR model, by including a quarantine state variable and evaluating the effect of preventative interventions [31]. We also formulate a fractional biological problem to mitigate the quantity of symptomatic infected populations with low and high risk with psychological difficulties. Key parameters for Covid-19, such as the disease-induced death rate as well as the basic reproductive ratio, are computed in a relatively accurate method. Both direct and indirect pieces of evidence are used to anticipate and validate the extensively discussed ending time, inflection point and total infected cases in big cities and other areas. In addition, the outbreak's start date has been estimated using inverse inference. Other hotspots throughout the globe are still being investigated.

The paper organization is given as: preliminaries is given in Section 2. The mathematical model formulation of the model is given in Section 3. The existence and uniqueness solution of the model is presented in Section 4. The Stability analysis is investigated in Section 5. Numerical analysis is presented in Section 6. The numerical simulation and discussion are provided in Section 7. Concluding remarks are summarized in Section 8.

## 2. Preliminaries

Here, we give some definitions and notations of fractional operators [11,13] that are utilized in this paper.

**Definition 2.1.** The two parametric Mittag-Leffler function  $m$  is denoted by  $E_{u,u_1}(m)$  and is defined as:

$$E_{u,u_1}(m) = \sum_{k=0}^{\infty} \frac{m^k}{\Gamma(uk + u_1)}, \quad u, u_1 > 0, m \in \mathbb{C}. \quad (2.1)$$

**Remark 2.1.** If  $u_1 = 1$ , then Eq. (2.1) converted into one parametric Mittag-Leffler function  $E_{u,1}(m) = E_u(m)$ , and if  $u = u_1 = 1$ , then  $E_{1,1}(m) = E_1(m) = e^x$ ,  $x \in \mathbb{R}^+$ .

**Remark 2.2.** The relationship between Gamma and Mittag-Leffler function is given as:

$$E_{u,u_1}(m) = mE_{u,u+u_1}(m) + \frac{1}{\Gamma(u_1)}. \quad (2.2)$$

**Definition 2.2.** The Sobolev space is denoted by  $H^1(a_1, a_2)$  and is given as

$$H^1(a_1, a_2) = \{q \in L^2 : q' \in L^2(a_1, a_2), a_1 < a_2\}. \quad (2.3)$$

**Definition 2.3.** Riemann–Liouville (RL) fractional derivative of the function  $m : \mathbb{R}^+ \rightarrow \mathbb{R}^+$  is defined as

$${}^a RL D_t^\alpha m(t) = \frac{d^n}{dt^n} \frac{1}{\Gamma(n-\alpha)} \int_a^t (t-s)^{\alpha-1} m(s) ds, \quad t > 0, \alpha \in (n-1, n). \quad (2.4)$$

**Definition 2.4.** Caputo (C) fractional derivative of the function  $m \in C^n$  is defined as

$${}^C D_t^\alpha m(t) = \frac{1}{\Gamma(n-\alpha)} \int_a^t (t-s)^{\alpha-1} m^{(n)}(s) ds, \quad \alpha \in (n-1, n] \text{ for } n \in \mathbb{Z}^+. \quad (2.5)$$

**Definition 2.5.** Atangana–Baleanu–Riemann–Liouville (ABRL) and Atangana–Baleanu–Caputo (ABC) fractional derivatives are defined as

$${}^{ABRL} D_t^\alpha M(t) = \frac{ABC(u)}{1-u} \frac{d}{dt} \int_a^t E_u \left( -\frac{u}{1-u} (t-s)^\alpha \right) M(s) ds, \quad (2.6)$$

$${}^{ABC} D_t^\alpha M(t) = \frac{ABC(u)}{1-u} \int_a^t E_u \left( -\frac{u}{1-u} (t-s)^\alpha \right) M'(s) ds, \quad (2.7)$$

where  $t > 0, u \in (0, 1], M \in H^1(a_1, a_2)$ , and  $ABC(u)$  is the normalized function.

**Remark 2.3.** If  $u = 0, 1$ , then from Eq. (2.7) we have  $ABC(0) = ABC(1) = 1$ .

**Definition 2.6.** Atangana–Baleanu–Caputo (ABC) fractional integral is given as

$$\begin{aligned} {}^a ABC I_t^\alpha M(t) &= \frac{1-u}{ABC(u)} M(t) + \frac{u}{D_1} \int_a^t (t-s)^{\alpha-1} M(s) ds, \quad t > 0, D_1 \\ &= ABC(u) \Gamma(u). \end{aligned} \quad (2.8)$$

**Remark 2.4.** Let  $0 < u \leq 1$  &  $g \in C([0, T], \mathbb{R}_+)$ . Then the one-step b.v.p. in ABC fractional operator:  ${}^a ABC D_t^\alpha M(t) = g(t)$ , for  $t \in [0, T]$  and  $M(0) = M_0$  possesses a unique solution given as below:

$$M(t) = M_0 + \frac{1-u}{ABC(u)} f(t) + \frac{u}{D_1} \int_a^t (t-s)^{\alpha-1} g(s) ds. \quad (2.9)$$

**Definition 2.7.** Laplace transformation of Eq. (2.7) is given as

$$\mathcal{L}\{ {}^a ABC D_t^\alpha M(t) \}(s) = \frac{ABC(u)[s^\alpha \mathcal{L}\{M(t)\}(s) - s^{\alpha-1} M(0)]}{u + s^\alpha(1-u)}. \quad (2.10)$$

### 3. Mathematical model formulation

To construct the system, we divide the Covid-19 grouped human population into five classes such as susceptible  $S$ , exposed  $E$ , infectious  $I$ , quarantined  $Q$  and recovered  $R$ . The complete human population is given by  $Z = S + E + I + Q + R$ . The mathematical model related to the ordinary derivative is as follows:

$$\begin{aligned} \frac{dS}{dt} &= \Pi - \beta SI - \mu S, \\ \frac{dE}{dt} &= \beta SI - (\gamma + \mu) E, \\ \frac{dI}{dt} &= \gamma E - (\delta + \mu) I + (1-p)\phi Q, \\ \frac{dQ}{dt} &= \delta I - (p\phi + \mu) Q, \\ \frac{dR}{dt} &= \phi Q - \mu R. \end{aligned} \quad (3.1)$$

In the proposed model (3.1),  $\Pi$  is the new upcoming arrival, infection rate is consider to be  $\beta$ ,  $\gamma$  is the latent time,  $\delta$  is the quarantine time,  $p$  is the total number of Covid-19 patients,  $\phi$  is the cure time and

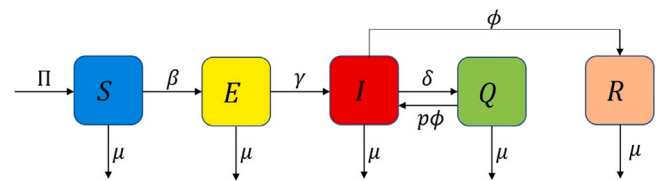


Fig. 1. Dynamical transmission of Covid-19.

Table 1

Biological parameters with the explanation as well as numerical ranges.

Parameter	Description	Values range	Sources
$\Pi$	Arrival rate of human population	1340	[32]
$\beta$	Transmission rate of infection	1.0	[10]
$\mu$	Humans natural death rate	0.172	[32]
$\gamma$	Latent time rate	0.5	[10]
$\delta$	Quarantine rate	0.15	[32]
$p$	Covid-19 fraction rate	0.3	Computed
$\phi$	Cure time rate	0.2	Computed

$\mu$  is the natural mortality rate. The dynamical transmission of Covid-19 is depicted in Fig. 1 The Table 1 below provides the base lines. The rate flows from the susceptible to exposed classes of hosts populations depend on the dynamical transmission of  $\beta$ ,  $\gamma$  is the rate flow from exposure to infectious class,  $\delta$  is the rate flow from infectious to quarantined class and  $\phi$  is the rate flow from quarantined to recovered class. In each class,  $\mu$  is the natural death rate that is going out respectively. The RL to Caputo operator is substituted by the fractional-order derivative. The key advantage of employing the Caputo fractional derivative is that the traditional initial conditions may be used without running into any issues during the solvability test. The fundamental problem with the aforementioned model is a dimension mismatch between the two sides. This can be resolved by altering the matching derivatives of the parameters with dependent on time. Thus, the dimension mismatch of the above-proposed model (3.1) is resolved as follows:

$$\begin{aligned} {}^C_0 D_t^\alpha S &= \Pi^\alpha - \beta^\alpha SI - \mu^\alpha S, \\ {}^C_0 D_t^\alpha E &= \beta^\alpha SI - (\gamma^\alpha + \mu^\alpha) E, \\ {}^C_0 D_t^\alpha I &= \gamma^\alpha E - (\delta^\alpha + \mu^\alpha) I + ((1-p)\phi)^\alpha Q, \\ {}^C_0 D_t^\alpha Q &= \delta^\alpha I - ((p\phi)^\alpha + \mu^\alpha) Q, \\ {}^C_0 D_t^\alpha R &= \phi^\alpha Q - \mu^\alpha R. \end{aligned} \quad (3.2)$$

The value of  $\alpha \in (0, 1)$ . Furthermore,  ${}^C_0 D_t^\alpha r(t)$ , is the Caputo fractional-order derivative.

The value of  $\alpha$  or to use Caputo's derivative is more significant than the order. The fundamental disadvantage of fractionalization is that when we use two or more compartmental models, a departing mass flux is equivalent to an incoming for the subsequent quantity of the class. As a result, the outgoing mass that transfer with certain fractional-order derivative can't appear in other class as an incoming mass without breaking the law of mass balance. For instance, the infected host populations in model (3.2) are in fractional time with the dimension  $(time)^{-\alpha}$ .

Therefore, a novel infected host with rate  $(time)^{-\alpha}$  is produced by the vulnerable human population with dimension  $(time)^{-\alpha}$ , which is in fractional  $t$ . As a result, the situation of mass balance results in inconsistency for the Covid-19 model system (3.2). Therefore, fractionalizing the multi compartmental system is not conceivable by switching the non-fractional to the fractional operators in the Covid-19 model's left-side quantities (3.2).

In addition, preventing the mismatch of dimensions is another issue with fractionalizing a compartmental Covid-19 model. In this instance, the writers converted each parameter's rate to its matching fractional order. Therefore, we have solid evidence that the dynamics of a power-law type govern the spread of infection. Therefore, the

random transmission process shouldn't include fractional  $t$  dynamics in the recruitment of babies or the death process. To avoid the dimension mismatch, the approach used in the model (3.2) does not resolve this problem. This problem was dealt with appropriately.

The drawback of the fractionalized model (3.2) regarding mass flux of compartment and fractionalization of the Covid-19 model to avoid the dimension mismatch has been observed. Here, the researchers changed rate of biological parameters pertaining to their fractional-order derivative. The approach to fractionalize the proposed model (3.1) is given as follows:

$$\begin{aligned} \frac{dS}{dt} &= \Pi \varphi_{11} \frac{(t-\tau)^{\varphi_{11}-1}}{\Gamma(\varphi_{11})} - \beta \varphi_{12} {}^{RL}D_t^{1-\varphi_{12}} SI - \mu \varphi_{13} {}^{RL}D_t^{1-\varphi_{13}} S, \\ \frac{dE}{dt} &= \beta \varphi_{12} {}^{RL}D_t^{1-\varphi_{12}} SI - \gamma \varphi_{22} {}^{RL}D_t^{1-\varphi_{22}} E - \mu \varphi_{23} {}^{RL}D_t^{1-\varphi_{23}} E, \\ \frac{dI}{dt} &= \gamma \varphi_{22} E - (\delta \varphi_{32} + \mu \varphi_{33}) I + ((1-p)\phi)^{\varphi_{34}} Q, \\ \frac{dQ}{dt} &= \delta \varphi_{32} I - ((p\phi)^{\varphi_{34}} + \mu \varphi_{43}) Q, \\ \frac{dR}{dt} &= \phi \varphi_{34} Q - \mu \varphi_{52} R. \end{aligned} \tag{3.3}$$

Thus, the mobility as well as mortality in hosts doesn't show in the domain of fractional calculus. Thus we take  $\varphi_{11} = \varphi_{13} = \varphi_{22} = \varphi_{23} = \varphi_{32} = \varphi_{33} = \varphi_{34} = \varphi_{43} = \varphi_{52} = 1$  and we will only follow a similar rule for the host during the transmission process, that is why we will take  $0 < \varphi_{12} < \alpha < 1$ . By the use of these points to the system (3.3), we have Covid-19 system with fractional calculus as follows:

$$\begin{aligned} \frac{dS}{dt} &= \Pi - \beta {}^{\alpha} {}^{RL}D_t^{1-\alpha} SI - \mu S, \\ \frac{dE}{dt} &= \beta {}^{\alpha} {}^{RL}D_t^{1-\alpha} SI - \gamma E - \mu E, \\ \frac{dI}{dt} &= \gamma E - (\delta + \mu) I + ((1-p)\phi) Q, \\ \frac{dQ}{dt} &= \delta I - ((p\phi) + \mu) Q, \\ \frac{dR}{dt} &= \phi Q - \mu R. \end{aligned} \tag{3.4}$$

It is evident from the model (3.4) that every equation's fractional operators take the RL form on the right-hand side. We are aware that the fractional Riemann-Liouville derivative of a constant function is non-zero. We might encounter difficulties in demonstrating the boundedness of the variables as a result of this flaw in the RL fractional operator. The beginning value problem in the RL fractional operator does not just depend on integer-order derivatives, which is another well-known phenomenon. For the shortcoming of the RL operator, we look difficulties by demonstrating the boundedness of state variables. The two big shortcoming of the RL derivatives are resolved by Caputo fractional-order derivative. Therefore, the relation between the RL and C's operator of the state variables is given as below:

$${}^{RL}D_t^{1-\alpha} B_t = {}^C D_t^{1-\alpha} B_t + \frac{B(0)t^{\alpha-1}}{\Gamma(\alpha)}. \tag{3.5}$$

By the use of expression (3.5), the system (3.4) gives

$$\begin{aligned} \frac{dS}{dt} &= \Pi - \beta {}^{\alpha} {}^{RL}D_t^{1-\alpha} SI - \mu S - \frac{\beta {}^{\alpha} S(0)I(0)t^{\alpha-1}}{\Gamma(\alpha)}, \\ \frac{dE}{dt} &= \beta {}^{\alpha} {}^{RL}D_t^{1-\alpha} SI - \gamma E - \mu E + \frac{\beta {}^{\alpha} S(0)I(0)t^{\alpha-1}}{\Gamma(\alpha)}, \\ \frac{dI}{dt} &= \gamma E - (\delta + \mu) I + ((1-p)\phi) Q, \\ \frac{dQ}{dt} &= \delta I - ((p\phi) + \mu) Q, \\ \frac{dR}{dt} &= \phi Q - \mu R. \end{aligned} \tag{3.6}$$

The model (3.6) is ill-defined in this case because it features a type second finite-time singularity at time  $t = 0$ . This singularity happens at a  $t = 0$  by the application of a fractional Riemann-Liouville derivative. However, in Caputo fractional derivative, this singularity at a moment of zero does not take place. As a result, the definitions of the

Riemann-Liouville and Caputo fractional derivatives become similar as the time approaches infinity and  $\alpha$  is between 0 and 1. As a result, both definitions produce the same results when used to study the behavior of values in an equilibrium zone throughout a dynamic process.

The work of the stability analysis of various dynamical systems was proven by many researchers [33]. The prime aim of our work is to identified the value near about equilibrium states of the system (3.6) in the long term of behavior. Thus, we eliminate the decaying term that depends on  $t$  R.H.S. of the system (3.6). Thus, the time-dependent differential equation with the C operators is given as follows:

$$\begin{aligned} {}^C D_t^{\alpha} S &= \Pi - \beta {}^{\alpha} {}^{RL}D_t^{1-\alpha} SI - \mu S, \\ {}^C D_t^{\alpha} E &= \beta {}^{\alpha} {}^{RL}D_t^{1-\alpha} SI - \gamma E - \mu E, \\ {}^C D_t^{\alpha} I &= \gamma E - (\delta + \mu) I + ((1-p)\phi) Q, \\ {}^C D_t^{\alpha} Q &= \delta I - ((p\phi) + \mu) Q, \\ {}^C D_t^{\alpha} R &= \phi Q - \mu R. \end{aligned} \tag{3.7}$$

The Banach space  $B$  of the continuous mappings defined on the interval  $L$  with the below form.

$$\|S, E, I, Q, R\| = \|S\| + \|E\| + \|I\| + \|Q\| + \|R\|. \tag{3.8}$$

In the Eq. (3.8) [34], we have

$$\begin{aligned} \|S\| &= \sup\{S(t) : t \text{ in } M\}, \\ \|E\| &= \sup\{E(t) : t \text{ in } M\}, \\ \|I\| &= \sup\{I(t) : t \text{ in } M\}, \\ \|Q\| &= \sup\{Q(t) : t \text{ in } M\}, \\ \|R\| &= \sup\{R(t) : t \text{ in } M\}. \end{aligned}$$

Also,  $B = 5 \times F(M)$ , and  $F(M)$  is the mappings in  $M$  with the supremum norm.

Therefore, system (3.7) at zero time doesn't have any singularity. The stability analysis by the use of expression  $|\arg \lambda_i| > \frac{\pi}{2n}$  for  $i = 1, 2, 3, \dots, m(\alpha_1 + \alpha_2 + \dots + \alpha_5)$  of the model (3.7) in the analysis portion.

The mathematical model related to the ABC fractional-order derivative is as follows:

$$\begin{aligned} {}^{ABC} D_t^{\alpha} S &= \Pi - \beta SI - \mu S, \\ {}^{ABC} D_t^{\alpha} E &= \beta SI - (\gamma + \mu) E, \\ {}^{ABC} D_t^{\alpha} I &= \gamma E - (\delta + \mu) I + (1-p)\phi Q, \\ {}^{ABC} D_t^{\alpha} Q &= \delta I - (p\phi + \mu) Q, \\ {}^{ABC} D_t^{\alpha} R &= \phi Q - \mu R. \end{aligned} \tag{3.9}$$

with i.c's

$$S(0) = S_0 > 0, E(0) = E_0 \geq 0, I(0) = I_0 \geq 0,$$

$$Q(0) = Q_0 \geq 0, R(0) = R_0 \geq 0.$$

### 3.1. Positively invariant region

To demonstrate the system (3.9) epidemiologically well-posed, we have proved the following theorem.

**Theorem 3.1.** *The set  $\Omega = \{(S, E, I, Q, R) \in \mathbb{R}_+^6 : Z \leq \Pi/\mu\}$  is positive non-variant for system (3.9).*

**Proof.** The sum of the all equations of model (3.9) gives

$${}^{ABC} D_t^{\alpha} Z = \Pi - \mu(S + E + I + Q + R) \leq \Pi - \mu Z. \tag{3.10}$$

The solution of Eq. (3.10) is

$$\begin{aligned} Z \leq & \left[ \frac{ABC(u)}{ABC(u) + (1-u)\mu} Z(0) + \frac{(1-u)\Pi}{ABC(u) + (1-u)\mu} \right] E_{u,1}(-dt^u) \\ & + \frac{u\Pi}{ABC(u) + (1-u)\mu} E_{u,u+1}(-dt^u), \end{aligned} \tag{3.11}$$

where  $d = \frac{u\mu}{ABC(u)+(1-u)\mu}$ .

The Eq. (3.10) simplifies as

$$Z \leq \frac{\Pi}{\mu} + \frac{ABC(u)}{ABC(u)+(1-u)\mu} \left[ Z(0) - \frac{\Pi}{\mu} \right] E_u(-dt^u).$$

Hence,  $Z \leq \frac{\Pi}{\mu}$  as  $t \rightarrow \infty$ . Therefore, all solutions of system (3.9) with a positive i.c. in  $\Omega$  will stay in  $\Omega$ . Hence, the theorem is proved.

### 3.2. Equilibrium points

The equilibria are equating the L.H.S. of the system (3.9) equals zero after that, solving the new system of algebraic equations.

#### 3.2.1. Disease free equilibrium points

The Disease free equilibrium (DFE) is represented by  $E^f$  and is given as

$$E^f = (S^f, E^f, I^f, Q^f, R^f) = \left( \frac{\Pi}{\mu}, 0, 0, 0, 0 \right).$$

#### 3.2.2. Disease endemic equilibrium points

The Disease endemic equilibrium (DEE) is denoted by  $E^e$  and is given as

$$E^e = (S^e, E^e, I^e, Q^e, R^e),$$

with

$$S^e = \frac{(\gamma + \mu)(\delta + \mu)}{\beta\gamma}, E^e = \frac{(\delta + \mu)}{\gamma\beta} \left[ \frac{\Pi\beta\gamma}{(\gamma + \mu)(\delta + \mu)} - \mu \right],$$

$$I^e = \frac{1}{\beta} \left[ \frac{\Pi\beta\gamma}{(\gamma + \mu)(\delta + \mu)} - \mu \right], Q^e = \frac{\delta}{(\phi + \mu)\beta} \left[ \frac{\Pi\beta\gamma}{(\gamma + \mu)(\delta + \mu)} - \mu \right],$$

$$R^e = \frac{\phi\delta}{(\phi + \mu)\beta\mu} \left[ \frac{\Pi\beta\gamma}{(\gamma + \mu)(\delta + \mu)} - \mu \right].$$

### 3.3. Basic reproductive number

The Basic reproductive number ( $\mathcal{R}_0$ ) for the system (3.9) is determined by using the next-generation technique [34,35]. Suppose we have two state of infection  $F$  (without infection state) and  $V$  (with infection state). We have

$$F = \begin{bmatrix} 0 & \beta S \\ 0 & 0 \end{bmatrix}, V = \begin{bmatrix} \gamma + \mu & 0 \\ -\gamma & \delta + \mu \end{bmatrix}.$$

This implies

$$FV^{-1} = \frac{1}{(\gamma + \mu)(\delta + \mu)} \begin{bmatrix} -\beta S\gamma & \beta S(\gamma + \mu) \\ 0 & 0 \end{bmatrix}.$$

Therefore, we have

$$\mathcal{R}_0 = \sqrt{\frac{\Pi\beta\gamma}{\mu(\gamma + \mu)(\delta + \mu)}}.$$

We evaluate the basic reproduction number  $\mathcal{R}_0$  and it is seen that the diseases are epidemic if the threshold  $\mathcal{R}_0 > 1$  and the diseases is non-epidemic if  $\mathcal{R}_0 < 1$ . If  $\mathcal{R}_0 = 1$ , then the state of bifurcation occurs.

## 4. Existence and uniqueness of model

We use the fixed point technique to propose certain conditions along with the existence as well as uniqueness to the solution of system (3.9) are obtained. For the sake of simplicity the R.H.S. of system (3.9) set:

$$\begin{aligned} \mathcal{J}_1(t, S, E, I, Q, R) &= \Pi - \beta SI - \mu S, \\ \mathcal{J}_2(t, S, E, I, Q, R) &= \beta SI - (\gamma + \mu)E, \\ \mathcal{J}_3(t, S, E, I, Q, R) &= \gamma E - (\delta + \mu)I + (1-p)\phi Q, \\ \mathcal{J}_4(t, S, E, I, Q, R) &= \delta I - (p\phi + \mu)Q, \\ \mathcal{J}_5(t, S, E, I, Q, R) &= \phi Q - \mu R. \end{aligned} \tag{4.1}$$

and reformulate the system (3.9) as

$$\begin{cases} {}_0^{ABC} D_t^\mu \mathcal{V}(t) = \mathcal{J}(t, \mathcal{V}(t)), t \in \mathcal{H} = [0, T], u \in (0, 1], \\ \mathcal{V}(0) = \mathcal{V}_0 \geq 0, \end{cases} \tag{4.2}$$

where,

$$\mathcal{V}(t) = \begin{bmatrix} S(t) \\ E(t) \\ I(t) \\ Q(t) \\ R(t) \end{bmatrix}, \mathcal{V}(0) = \begin{bmatrix} S(0) \\ E(0) \\ I(0) \\ Q(0) \\ R(0) \end{bmatrix}, \mathcal{J}(t, \mathcal{V}(t)) = [\mathcal{J}_i(t, S, E, I, Q, R)], i = 1 \text{ to } 5. \tag{4.3}$$

By Eq. (2.9), the value of the fractional-order one-step boundary value problem (4.2) in the non-linear Volterra integral form is given as follows:

$$\mathcal{V}(t) = \mathcal{V}(0) + \frac{1-u}{ABC(u)} \mathcal{J}(t, \mathcal{V}(t)) + \frac{u}{D_1} \int_0^t (t-s)^{u-1} \mathcal{J}(s, \mathcal{V}(s)) ds. \tag{4.4}$$

Thus, for the case of investigation of solution existence, the system (3.9) along with the i.v.p. is equivalent to the system (4.2). Now, we define the Banach space  $\mathcal{Y} = C(\mathcal{H}, \mathbb{R}_+^5)$  w.r.t. sup. norm

$$\|\mathcal{V}(t)\| = \sup_{t \in \mathcal{H}} \{|\mathcal{V}| : \mathcal{V} \in \mathcal{Y}\}$$

where,  $\sup_{t \in \mathcal{H}} |\mathcal{V}(t)| = \sup_{t \in \mathcal{H}} [|S| + |E| + |I| + |Q| + |R|]$  and  $S, E, I, Q, R \in C(\mathcal{H}, \mathbb{R}_+^5)$ . So, by defining the mapping  $\mathcal{A} : \mathcal{Y} \rightarrow \mathcal{Y}$  as

$$\mathcal{A}[\mathcal{V}(t)] = \mathcal{B}_1[\mathcal{V}(t)] + \mathcal{B}_2[\mathcal{V}(t)] \tag{4.5}$$

where,

$$\mathcal{B}_1[\mathcal{V}(t)] = \mathcal{V}(0) + \frac{1-u}{ABC(u)} \mathcal{J}(t, \mathcal{V}(t)), \tag{4.6}$$

$$\mathcal{B}_2[\mathcal{V}(t)] = \frac{u}{D_1} \int_0^t (t-s)^{u-1} \mathcal{J}(v, \mathcal{V}(s)) ds. \tag{4.7}$$

The Eq. (4.4) reduced into the fixed point problem:

$$\mathcal{V}(t) = \mathcal{A}[\mathcal{V}(t)]. \tag{4.8}$$

Next, we have the below Lipschitz condition and non-linear function  $\mathcal{J} : \mathcal{H} \times \mathbb{R}_+^5 \rightarrow \mathbb{R}_+^5$  appeared in Eq. (4.4).

**Theorem 4.1.** *The model (3.9) in the form of Eq. (4.2). Then under the condition there exist  $M_J$  s.t. for  $t \in \mathcal{H}$ ,  $\mathcal{V}^*, \mathcal{V}^{**} \in \mathcal{Y}$  we have*

$$\|\mathcal{J}(t, \mathcal{V}^*(t)) - \mathcal{J}(t, \mathcal{V}^{**}(t))\| \leq M_J \|\mathcal{V}^*(t) - \mathcal{V}^{**}(t)\|,$$

holds with

$$\left[ \frac{1-u}{ABC(u)} + \frac{T^u}{D_1} \right] M_J < 1, \tag{4.9}$$

the Eq. (4.2) is equivalent to system (3.9) admits a unique solution to  $\mathcal{H}$ .

**Proof.** For considering  $t \in \mathcal{H}$ , let  $\mathcal{V}^*$  as well as  $\mathcal{V}^{**}$  be two solutions of Eq. (4.2) in  $\mathcal{Y}$ . Then

$$\begin{aligned} \left\| \mathcal{A}[\mathcal{V}^*(t)] - \mathcal{A}[\mathcal{V}^{**}(t)] \right\| &\leq \left| \frac{1-u}{ABC(u)} \sup_{t \in \mathcal{H}} N \right| + \left| \frac{u}{D_1} \sup_{t \in \mathcal{H}} \int_0^t (t-s)^{u-1} N ds \right|, \\ &\leq \frac{1-u}{ABC(u)} \|\mathcal{V}^*(t) - \mathcal{V}^{**}(t)\| + \frac{T^u}{D_1} \|\mathcal{V}^*(t) - \mathcal{V}^{**}(t)\|, \\ &= \left[ \frac{1-u}{ABC(u)} + \frac{T^u}{D_1} \right] M_J \|\mathcal{V}^*(t) - \mathcal{V}^{**}(t)\|. \end{aligned} \tag{4.10}$$

where,  $N = \mathcal{J}(t, \mathcal{V}^*(t)) - \mathcal{J}(t, \mathcal{V}^{**}(t))$ .

Therefore,  $\mathcal{A}$  is a contraction map for (4.9). Thus, the Eq. (4.4) has a unique integral. Hence, the dynamical system (3.9) gives a unique integral.

5. Ulam–Hyers stability

Here, we set up the Ulam–Hyers stability to analyse the model behaviour for dynamical system (3.9).

**Definition 5.1.** The proposed system (3.9) examined in the system (4.2) is known as Ulam–Hyers stable if there exists a positive value  $C_J$  with the below conditions:

for each positive number  $l$  and every value  $\mathcal{V}^* \in \mathcal{Y}$  satisfying the expression

$$\| {}_0^{ABC} D_t^\mu \mathcal{V}^*(t) - \mathcal{J}(t, \mathcal{V}^*(t)) \| \leq l, t \in H, \tag{5.1}$$

then,  $\exists$  a unique value  $\mathcal{V} \in \mathcal{Y}$  of system of Eq. (4.2) with expression  $\mathcal{V}(0) = \mathcal{V}^*(0)$  such that

$$\| \mathcal{V}^*(t) - \mathcal{V}(t) \| \leq C_J l, \forall t \in H, \tag{5.2}$$

with,

$$\mathcal{V}^*(t) = \begin{bmatrix} S^*(t) \\ E^*(t) \\ I^*(t) \\ Q^*(t) \\ R^*(t) \end{bmatrix}, \mathcal{V}^*(0) = \begin{bmatrix} S^*(0) \\ E^*(0) \\ I^*(0) \\ Q^*(0) \\ R^*(0) \end{bmatrix}, \mathcal{J}(t, \mathcal{V}^*(t)) = [\mathcal{J}_1(t, S^*, E^*, I^*, Q^*, R^*),]$$

$i=1$  to 5.

$$l = \max \begin{bmatrix} l_1 \\ l_2 \\ l_3 \\ l_4 \\ l_5 \end{bmatrix}, \text{ and } C_J = \max \begin{bmatrix} C_{J_1} \\ C_{J_2} \\ C_{J_3} \\ C_{J_4} \\ C_{J_5} \end{bmatrix}.$$

We refer to the number is  $C_J$  Ulam–Hyers stability constant.

**Lemma 5.1.** The solution  $\mathcal{V}_\zeta^*(t)$  for perturbed problem

$$\begin{cases} {}_0^{ABC} D_t^\mu \mathcal{V}_\zeta^*(t) = H(t, \mathcal{V}_\zeta^*(t)) + \zeta(t), \forall t \in H \\ \mathcal{V}_\zeta^*(0) = \mathcal{V}_0^* \end{cases} \tag{5.3}$$

satisfies the expression

$$\| \mathcal{V}_\zeta^*(t) - \mathcal{V}^*(t) \| \leq \mathcal{A}l, \tag{5.4}$$

where,  $\mathcal{V}_\zeta^*$  is the value of Eq. (5.4),  $\mathcal{V}^*$  satisfies Eq. (5.1) and  $\mathcal{A} = \left[ \frac{1-u}{ABC(u)} + \frac{T^u}{D_1} \right]$ .

**Theorem 5.2.** Consider the Lemma 5.1 and Eq. (5.3) and also further extended Ulam–Hyers stable in  $\mathcal{Y}$  if  $(1 - \mathcal{A}M_J) > 0$ . Then, the dynamical system (3.9) is Ulam–Hyers as well as further extended Ulam–Hyers stable in  $\mathcal{Y}$ .

**Proof.** Let  $\mathcal{V}^* \in \mathcal{Y}$  obeys the Eq. (5.1) and  $\mathcal{V}^*$  be the unique value of the system (4.2) with the basic expression  $\mathcal{V}(0) = \mathcal{V}^*(0)$  if and only if  $\mathcal{V}_0 = \mathcal{V}_0^*$ . Then from Remark 2.4 follows that

$$\mathcal{V}(t) = \mathcal{V}^* + \frac{1-u}{ABC(u)} \mathcal{J}(t, \mathcal{V}^*(t)) + \frac{u}{D_1} \int_0^t (t-s)^{u-1} \mathcal{J}(s, \mathcal{V}^*(s)) ds. \tag{5.5}$$

By Eq. (4.9) and Lemma 5.1, we have

$$\begin{aligned} \| \mathcal{V}^*(t) - \mathcal{V}(t) \| &\leq \sup_{t \in H} | \mathcal{V}^*(t) - \mathcal{V}_\zeta^*(t) | + \sup_{t \in H} | \mathcal{V}_\zeta^*(t) - \mathcal{V}(t) |, \\ &\leq 2\mathcal{A}l + \left[ \frac{1-u}{ABC(u)} + \frac{T^u}{D_1} \right] M_J \| \mathcal{V}^*(t) - \mathcal{V}(t) \|. \end{aligned} \tag{5.6}$$

Therefore, we have

$$\| \mathcal{V}^*(t) - \mathcal{V}(t) \| \leq \frac{2\mathcal{A}}{1 - \mathcal{A}M_J} l. \tag{5.7}$$

For,  $C_J = \frac{2\mathcal{A}}{1 - \mathcal{A}M_J}$  with  $1 - \mathcal{A}M_J > 0$ , the Eq. (5.7) gives

$$\| \mathcal{V}^*(t) - \mathcal{V}(t) \| \leq C_J l. \tag{5.8}$$

Thus, the solution to the fractional initial value problem (4.2) is Ulam–Hyers stable. Further, by taking,  $\mathcal{V}_J(l) = C_J l$  along with  $\mathcal{V}_J(0) = 0$  we have

$$\| \mathcal{V}^*(t) - \mathcal{V}(t) \| \leq W_J(l), \tag{5.9}$$

where,  $W_J : H \rightarrow \mathcal{R}_+^5$  with  $W_J(0) = 0$ . Therefore, the fractional initial value problem (4.2) is also the further extended Ulam–Hyers stable. Hence, the system (3.9) is both Ulam–Hyers as well as their further extended form.

6. Numerical analysis

Schemes in the Adams-Moulton family are implicit two-step methods that use the derivative evaluated at  $t_{i-1}$  plus prior points but only use the solution. The one-step Adams-Moulton method is the backward Euler scheme and the two-step method is the trapezoidal rule. But here in this section, we employed the two-step Adams-Bashforth-Moulton scheme for the proposed model (3.9) with Atangana-Baleanu fractional derivative in Caputo sense gives the below Volterra integral type equation

$$S(t) - S(0) = \frac{1-u}{ABC(u)} \mathcal{J}_1(t, S(t)) + \frac{u}{D_1} \int_0^t (t-s)^{u-1} \mathcal{J}_1(s, S(s)) ds. \tag{6.1}$$

At time  $t = t_i$  and  $t = t_{i+1}, i \in \mathbb{Z}^+$ , we have

$$S(t_i) - S(0) = \frac{1-u}{ABC(u)} \mathcal{J}_1(t_{i-1}, S(t_{i-1})) + \frac{u}{D_1} \int_0^{t_i} (t_i-t)^{u-1} \mathcal{J}_1(t, S(t)) dt,$$

and

$$S(t_{i+1}) - S(0) = \frac{1-u}{ABC(u)} \mathcal{J}_1(t_i, S(t_i)) + \frac{u}{D_1} \int_0^{t_{i+1}} (t_{i+1}-t)^{u-1} \mathcal{J}_1(t, S(t)) dt.$$

Also,

$$S(t_{i+1}) - S(0) = \frac{1-u}{ABC(u)} \left[ \mathcal{J}_1(t_i, S(t_i)) - \mathcal{J}_1(t_{i-1}, S(t_{i-1})) \right] + \frac{u}{D_1} (X_{u,1} - X_{u,2}) \tag{6.2}$$

where  $X_{u,1} = \int_0^{t_{i+1}} (t_{i+1}-t)^{u-1} \mathcal{J}_1(t, S) dt$  and  $X_{u,2} = \int_0^{t_i} (t_i-t)^{u-1} \mathcal{J}_1(t, S) dt$ .

For the interval  $[t, t_{k+1}]$ , the two step Lagrange polynomial is shown in the form

$$\mathcal{J}_1(t, S(t)) = \frac{t-t_{i-1}}{h} \mathcal{J}_1(t_i, S(t_i)) - \frac{t-t_i}{h} \mathcal{J}_1(t_{i-1}, S(t_{i-1})), \tag{6.3}$$

this means that

$$\begin{aligned} X_{u,1} &= \frac{\mathcal{J}_1(t_i, S(t_i))}{h} \left[ \frac{2ht_{i+1}^u}{u} - \frac{t_{i+1}^{u+1}}{u+1} \right] - \frac{\mathcal{J}_1(t_{i-1}, S(t_{i-1}))}{h} \left[ \frac{ht_{i+1}^u}{u} - \frac{t_{i+1}^{u+1}}{u+1} \right], \\ I_{u,2} &= \frac{\mathcal{J}_1(t_i, S(t_i))}{h} \left[ \frac{ht_i^u}{u} - \frac{t_i^{u+1}}{u+1} \right] - \frac{\mathcal{J}_1(t_{i-1}, S(t_{i-1}))}{h} \left[ \frac{ht_i^u}{u} - \frac{t_i^{u+1}}{u+1} \right]. \end{aligned} \tag{6.4}$$

By using Eq. (6.4) into (6.2) we get

$$S(t_{i+1}) = S(t_i) + \mathcal{J}_1(t_i, S(t_i)) \mathcal{A}_1(u) - \mathcal{J}_1(t_{i-1}, S(t_{i-1})) \mathcal{A}_2(u), \tag{6.5}$$

is the approximate value for  $S$  class of Eq. (4.3) with ABC fractional derivative in which

$$\mathcal{A}_j(u) = \begin{cases} \frac{1-u}{ABC(u)} + \frac{u}{hD_1} \left( \frac{2ht_{i+1}^u}{u} - \frac{t_{i+1}^{u+1}}{u+1} - \frac{ht_i^u}{u} + \frac{t_i^{u+1}}{u+1} \right) & \text{if } j = 1, \\ \frac{1-u}{ABC(u)} + \frac{u}{hD_1} \left( \frac{ht_{i+1}^u}{u} - \frac{t_{i+1}^{u+1}}{u+1} + \frac{t_i^{u+1}}{u+1} \right) & \text{if } j = 2. \end{cases} \tag{6.6}$$

In a similar manner, we can achieve the above-mentioned numerical scheme for the leftover five state of the system (3.9) as

$$E(t_{i+1}) = E(t_i) + \mathcal{J}_2(t_i, E(t_i)) \mathcal{A}_1(u) - \mathcal{J}_2(t_{i-1}, E(t_{i-1})) \mathcal{A}_2(u),$$

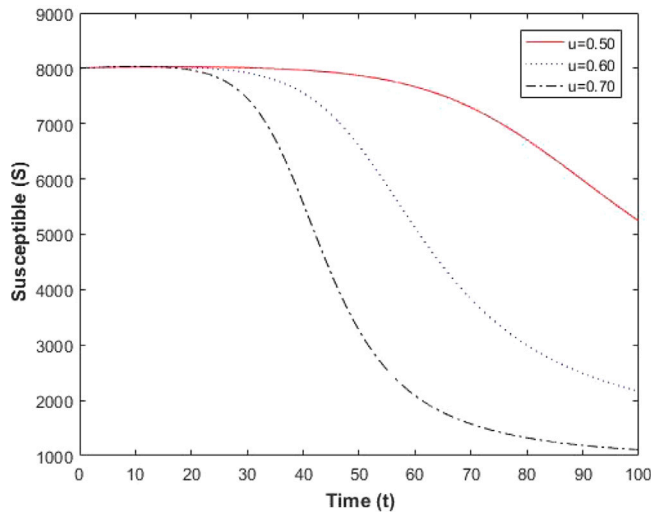


Fig. 2. Evolution of  $u$  on  $S$ .

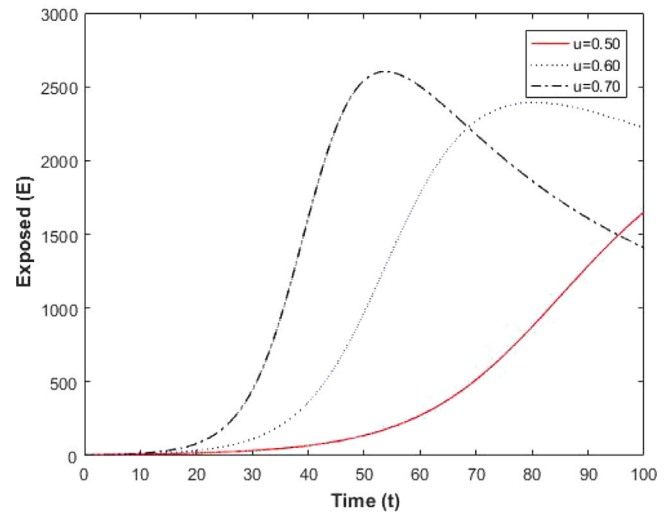


Fig. 3. Evolution of  $u$  on  $E$ .

$$I(t_{i+1}) = I(t_i) + \mathcal{J}_3(t_i, I(t_i))\mathcal{A}_1(u) - \mathcal{J}_3(t_{i-1}, I(t_{i-1}))\mathcal{A}_2(u),$$

$$Q(t_{i+1}) = Q(t_i) + \mathcal{J}_4(t_i, Q(t_i))\mathcal{A}_1(u) - \mathcal{J}_4(t_{i-1}, Q(t_{i-1}))\mathcal{A}_2(u),$$

$$R(t_{i+1}) = R(t_i) + \mathcal{J}_5(t_i, R(t_i))\mathcal{A}_1(u) - \mathcal{J}_5(t_{i-1}, R(t_{i-1}))\mathcal{A}_2(u).$$

7. Numerical simulation and discussion

The numerical simulation is presented with the help of computational software. Fig. 2 show the effect of ‘ $u = 0.50, 0.60, 0.70$ ’ on susceptible human  $S$  over  $t$ . In Fig. 2, it is seen that the population of susceptible humans mitigates initially as we increase ‘ $u$ ’ but it attains parallel to time value at  $t = 0 - 30$ . Fig. 3 show the effect of ‘ $u = 0.50, 0.60, 0.70$ ’ on exposed human  $E$  over time  $t$ . Fig. 3 shows that the population of  $E$  significantly increases as we increase ‘ $u$ ’ it also decreases with time after  $t = 50$ . Afterwards, Fig. 4 demonstrates the effects of  $u = 0.50, 0.60, 0.70$  on  $I$ . So, as we increase the value of  $u$ , the graph of  $I$  also increases. In Fig. 5, we seen the effect of  $u = 0.50, 0.60, 0.70$  on  $Q$  class. It is seen that ‘ $u$ ’ has negative effects on  $Q$ . Fig. 6 exhibits the effects of  $u = 0.50, 0.60, 0.70$  on  $R$ . Since, as we increase the value of  $u$ , the graph of  $I$  also increases. In Fig. 7, we seen the effect of  $u = 0.50, 0.60, 0.70$  on  $D$  class. It is seen that ‘ $u$ ’ has positive effects on  $D$ . Hence, Figs. 2 to 7 demonstrates the trajectory of the  $S, E, I, Q, R$  and  $D$  for three different values of  $u$ . It can be observed that the significant value of order  $u$  has an impact on the dynamic transmission of the illness. For instance, when the fractional index parameter decreases from  $0.7 - 0.5$ , the peak of the illness is lowered but the illness stays longer in the system with a decreased value of order  $u$ .

8. Conclusion

In this research paper, we proposed and analyzed a computational model to assess the impact of quarantine on the transmission dynamics of Covid-19 disease. The Atangana-Baleanu Covid-19 mathematical model is performed and the system is qualitatively and quantitatively analyzed. We have explored the impact of quarantine on the infected population. Our simulation results demonstrate that quarantine of the infected population is more effective in controlling and breaking the Covid-19 spread chain. This model incorporates properly the intrinsic effects of hidden infectious as well as exposed classes on the total affected population. The new quarantined class, together with the recovery and death variables have been introduced into the classical SEIR epidemic model. Further, we estimate a lot of key biological parameters for the Covid-19 model, like the quarantine latent as well

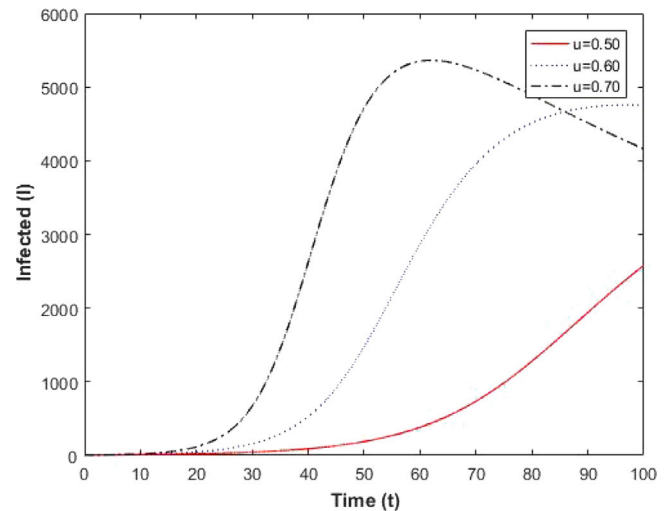


Fig. 4. Evolution of  $u$  on  $I$ .

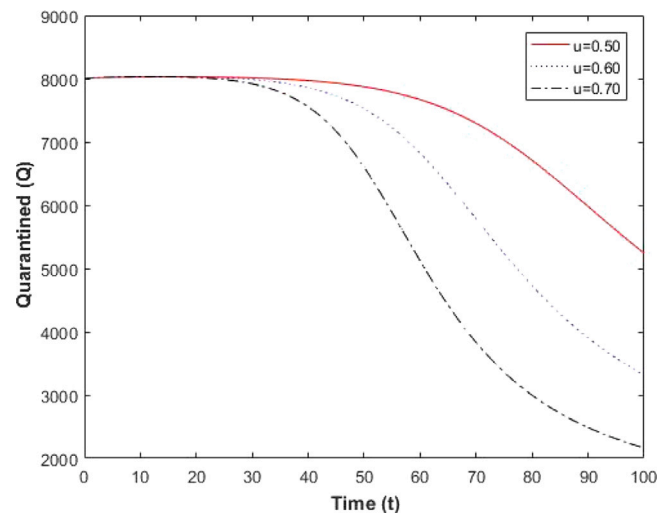


Fig. 5. Evolution of  $u$  on  $Q$ .

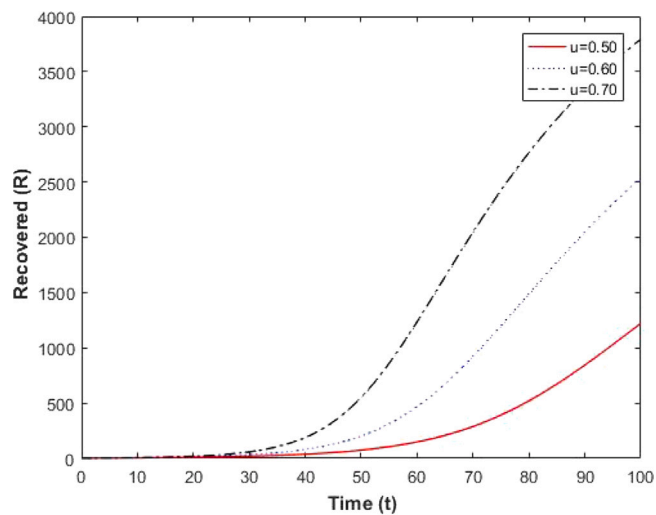


Fig. 6. Evolution of  $u$  on  $R$ .

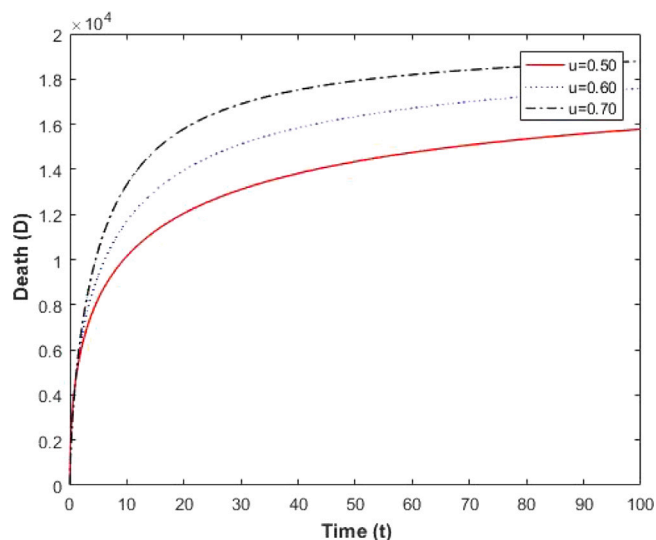


Fig. 7. Evolution of  $u$  on  $D$ .

as  $\mathcal{R}_0$  in a relatively reliable way to estimate the possible inflection point. However, the lack of knowledge on the first infected case has inverse inference for understanding the spread of the Covid-19 model and preventing similar kinds of virus in the upcoming days.

#### Concluded remark

We evaluate the basic reproduction number  $\mathcal{R}_0$  and established a Ulam-Hyers stability analysis. It is seen that DFE is locally asymptotically stable when  $\mathcal{R}_0 < 1$  as well as unstable if  $\mathcal{R}_0 > 1$ . Figures demonstrate the impact of fractional order  $\alpha$ . Atangana-Baleanu-Caputo is discovered to have even better results in terms of stability analysis than the other fractional operators in the numerical simulation.

#### Highlights

A computational model of the Covid-19 pandemic is proposed and studied. The Covid-19 model has a big biological parameter such as the Covid-19 fraction rate. The fractional operator  $\alpha$  demonstrates the effect in which we discuss a special case when making basic reproductive ratio  $\mathcal{R}_0 < 1$  is no longer a sufficient condition for the eradicate of the

illness, however, this condition is necessary. Our proposed model gives computation of various key biological parameters like reproduction number, quarantine rate and Covid-19 fraction rate which are really useful information for medical practitioners to understand the prediction and control of transmission dynamics of the disease. Moreover, the model and simulation are very helpful experimental tool for testing and estimating the biological parameters values used in the proposed model. We used the two-step ABM predictor-corrector approach to roughly identify the Covid-19 pandemic's origin.

#### Future direction

For future work, it would be interesting to come out with an extension of our proposed SEIQR by adding suitable state variables, that take an important role to control the Covid-19 spread. Hence, with the development of new kinds of vaccines to mitigate the Covid-19 effects, it will be important to study the impact of the vaccine campaign on the optimal behavior of our proposed model.

#### Data availability

The datasets and code are provided: <https://github.com/RamSingh12345678/Matlab-program-for-a-fractional-Model.git>.

#### Declaration of competing interest

The authors declare that they have no known competing financial interests or personal relationships that could have appeared to influence the work reported in this paper.

#### References

- [1] F. Bozkurt, Yousef Ali, D. Baleanu, et al., A mathematical model of the evolution and spread of pathogenic coronaviruses from natural host to human host, *Chaos Solit. Fractals*. 138 (2020) 109931.
- [2] Organization WH, WHO Coronavirus disease(Covid-19) situation report-198; data as received by WHO from national authorities, in: CEST, 2020.
- [3] Organization WH, WHO press release, 2020, Archived from the original on 11 2020. Retrieved 12 2020.
- [4] Y. Zhang, L. Rong, X. Li, et al., MedSeq2Seq: A medical knowledge enriched sequence to sequence learning model for Covid-19 diagnosis, in: IEEE International Conference on Bioinformatics and Biomedicine, BIBM, 2021, pp. 3181–3184, <http://dx.doi.org/10.1109/BIBM52615.2021.9669854>.
- [5] N.I. Okposo, M.O. Adewole, E.N. Okposo, et al., A mathematical study on a fractional Covid-19 transmission model within the framework of nonsingular and nonlocal kernel, *Chaos Solit. Fractals*. 152 (2021) 111427.
- [6] M.V. Madhavan, A. Khamparia, D. Gupta, et al., Res-CovNet: an internet of medical health things driven Covid-19 framework using transfer learning, *Neural Comput. Appl.* (2021) <http://dx.doi.org/10.1007/s00521-021-06171-8>.
- [7] H. Su, D. Zhao, H. Elmannai, et al., Multilevel threshold image segmentation for Covid-19 chest radiography: A framework using horizontal and vertical multiverse optimization, *Comput. Biol. Med.* (2022) 105618.
- [8] A. Qi, D. Zhao, F. Yu, et al., Directional mutation and crossover boosted ant colony optimization with application to Covid-19 X-ray image segmentation, *Comput. Biol. Med.* (2022) 105810.
- [9] M.A. Khan, A. Atangana, Modeling the dynamics of novel coronavirus (2019-nCov) with fractional derivative, *Alex Eng J.* 59 (4) (2020) 2379–2389.
- [10] A.U. Rehman, R. Singh, Agarwal P., Modeling, analysis and prediction of new variants of Covid-19 and dengue co-infection on complex network, *Chaos Solit. Fractals*. 150 (2021) 111008.
- [11] I. Podlubny, *Fractional Differential Equations*, Mathematics in Science and Engineering, Academic Press, New York, NY, USA, 1999.
- [12] M. Caputo, M. Fabrizio, A new definition of fractional derivative without singular kernel, *Prog. Fract. Differ. Appl.* 2 (2015) 73–85.
- [13] A. Atangana, D. Baleanu, New fractional derivatives with nonlocal and non-singular kernel: theory and application to heat transfer model, *Therm. Sci.* 20 (2) (2016) 763–769.
- [14] P. Agarwal, R. Singh, A.U. Rehman, Numerical solution of a hybrid mathematical model of dengue transmission with relapse and memory via Adam-Bashforth-Moulton predictor-corrector, *Chaos Solit. Fractals*. 143 (2021) 110564.
- [15] A.U. Rehman, R. Singh, T. Abdeljawad, et al., Modeling, analysis and numerical solution to malaria fractional model with temporary immunity and relapse, *Adv. Diff. Equ.* 2021 (2021) 390.

- [16] O. Samuel, A.B. Omojo, S.M. Mohsin, et al., An Anonymous IoT-Based E-Health Monitoring System Using Blockchain Technology, *IEEE Systems Journal*, <http://dx.doi.org/10.1109/JSYST.2022.3170406>.
- [17] Z. Wu, S. Xuan, J. Xie, et al., How to ensure the confidentiality of electronic medical records on the cloud: A technical perspective, *Comput. Biol. Med.* 147 (2022) 105726.
- [18] N. Sharma, R. Singh, J. Singh, et al., Modeling assumptions, optimal control strategies and mitigation through vaccination to zika virus, *Chaos Solit. Fractals*. 150 (2021) 111137.
- [19] N. Sharma, R. Pathak, R. Singh, Modeling of media impact with stability analysis and optimal solution of SEIRS epidemic model, *J. Interdiscip. Math.* 22 (7) (2019) 1123–1156.
- [20] N. Sharma, R. Singh, C. Cattani, et al., Modeling and complexity in dynamics of T-cells and cytokines in dengue fever based on antiviral treatment, *Chaos Solit. Fractals*. 153 (2) (2021) 11448.
- [21] R. Singh, N. Sharma, Ghosh A., Modeling assumptions, mathematical analysis and mitigation through intervention: An application to ebola type infectious disease, *Lett. Biomath.* 6 (2) (2019) 1–19.
- [22] L. He, P. Tiwari, R. Su, et al., CovidNet: An automatic architecture for Covid-19 detection with deep learning from chest X-ray images, *IEEE Internet Things J.* 9 (13) (2022) 11376–11384.
- [23] J. Jajarmi, B. Ghanbari, D. Baleanu, A new and efficient numerical method for the fractional modeling and optimal control of diabetes and tuberculosis co-existence, *Chaos* 29 (9) (2019) 093111.
- [24] Y. Belgaid, M. Helal, A. Lakmeche, et al., A mathematical study of a coronavirus model with the Caputo fractional-order derivative, *Fract. Fract.* 5 (2021) 87.
- [25] E.A. Rashed, S. Koderia, A. Hirata, Covid-19 forecasting using new viral variants and vaccination effectiveness models, *Comput. Biol. Med.* 149 (2022) 105986.
- [26] K. Shankar, E. Perumal, P. Tiwari, et al., Deep learning and evolutionary intelligence with fusion-based feature extraction for detection of Covid-19 from chest X-ray images, *Multimedia Syst.* 28 (2022) 1175–1187.
- [27] K. Shankar, E. Perumal, V.G. Díaz, et al., An optimal cascaded recurrent neural network for intelligent Covid-19 detection using Chest X-ray images, *Appl. Soft Comput.* (ISSN: 1568-4946) (2021) 113, <http://dx.doi.org/10.1016/j.asoc.2021.107878>.
- [28] A.A. Hamou, E. Azroul, L. Alaoui, Fractional model and numerical algorithms for predicting Covid-19 with isolation and quarantine strategies, *Int. J. Appl. Comput. Math.* 7 (2021) 142.
- [29] D. Shome, T. Kar, S.N. Mohanty, et al., Covid-transformer: Interpretable Covid-19 detection using vision transformer for healthcare, *Int. J. Environ. Res. Public Health* 18 (21) (2021) 11086.
- [30] A. Atangana, K.M. Owolabi, New numerical approach for fractional differential equations, *Math. Model Nat. Phenom.* (2018) 13.
- [31] S. He, Y. Peng, K. Sun, SEIR modeling of the Covid-19 and its dynamics, *Nonlinear Dynam.* 101 (2020) 1667–1680.
- [32] O. Samuel, et al., IoMT: A Covid-19 Healthcare System driven by Federated Learning and Blockchain, *IEEE Journal of Biomedical and Health Informatics*, <http://dx.doi.org/10.1109/JBHI.2022.3143576>.
- [33] K. Hu, et al., Colorectal polyp region extraction using saliency detection network with neutrosophic enhancement, *Comput. Biol. Med.* (2022) 105760.
- [34] A.U. Rehman, R. Singh, J. Singh, Mathematical analysis of multi-compartmental malaria transmission with reinfection, *Chaos Solit. Fractals* 163 (2) (2022) 112527.
- [35] DP. Van den, J. Watmough, Reproduction numbers and sub-threshold endemic equilibria for compartmental models of disease transmission, *Math. Biosci.* 180 (2002) 29–48.